WOOD RECOGNITION BASED ON TERAHERTZ SPECTRUM AND HYPERSPECTRAL TECHNOLOGY

Xing Da Yun, Yuan Wang*, Wen Jin Ma, Lei Zhao

School of Technology, Beijing Forestry University, Beijing, China;
Key Lab of State Forestry and Grassland Administration for Forestry Equipment and Automation, Beijing, China;
Research Center for Biodiversity Intelligent Monitoring, Beijing Forestry University, Beijing, China; e-mail: wangyuan@bjfu.edu.cn

Terahertz time-domain spectroscopy (THz-TDS) and hyperspectral technology were used for wood recognition. As wood is a valuable national resource, it is essential to utilize it efficiently and reasonably by classifying the species of wood. To accomplish this, ten distinct species of wood, including five types of softwood (Pinus sylvestris, Pinus tabulaeformis, Pinus massoniana, Larix gmelinii, and Pinus koraiensis) and five types of hardwood (Xylosma racemosum, Populus davidiana, Fraxinus rhynchophylla, Betula platyphylla, and Tilia tuan Szyszyl), were selected as experimental samples. Four hundred groups of data for terahertz absorption coefficient spectra and four hundred groups of hyperspectral data were acquired using THz-TDS and hyperspectral technology, respectively, and then examined for their spectral features. Three spectral preprocessing techniques, including the Savitsky–Golay smoothing algorithm, standard normal variable transformation, and multivariate scattering correction, were employed to preprocess the spectrum. Support vector machine recognition models were then created to compare and analyze the effects of recognition. The results demonstrated that both THz-TDS and hyperspectral approaches could successfully identify five different species of hardwood from various families and genera, with the highest accuracy rates of 92 and 94%, respectively. THz-TDS achieved a 92% recognition rate for five different species of softwood from the same family, indicating good recognition effects, while hyperspectral technology did not achieve such results.

Keywords: *THz spectroscopy, hyperspectral technology, support vector machine, hardwood, softwood.*

РАСПОЗНАВАНИЕ СОРТОВ ДРЕВЕСИНЫ С ИСПОЛЬЗОВАНИЕМ ТЕРАГЕРЦОВОГО СПЕКТРА И ГИПЕРСПЕКТРАЛЬНОЙ ТЕХНОЛОГИИ

X. Yun, Y. Wang*, W. Ma, L. Zhao

УДК 543.42:661.728.36

Пекинский университет лесного хозяйства, Пекин, Китай;
Государственное управление лесного хозяйства и пастбищ лесохозяйственной техники и автоматизации, Пекин, Китай;
Исследовательский центр интеллектуального мониторинга биоразнообразия Пекинского университета лесного хозяйства, Пекин, Китай; e-mail: wangyuan@bjfu.edu.cn

(Поступила 13 декабря 2022)

Для распознавания сортов древесины использованы терагерцовая спектроскопия во временной области (THz-TDS) и гиперспектральная технология. Десять образцов древесины различных пород, в том числе пять видов хвойных (Pinus sylvestris, Pinus tabulaeformis, Pinus massoniana, Larix gmelinii и Pinus koraiensis) и пять видов лиственных (Xylosma racemosum, Populus davidiana, Fraxinus rhynchophylla, Betula platyphylla и Tilia tuan Szyszyl), выбраны в качестве экспериментальных. Исследование спектральных характеристик проведено на наборах из 400 ТГц-спектров поглощения и гиперспектральных данных. Использованы три метода предварительной обработки спектра: алгоритм сглаживания Савицкого–Голея, стандартное нормальное переменное преобразование и коррекция

многомерного рассеяния. Созданы модели распознавания методом опорных векторов и анализа эффектов распознавания. Показано, что с помощью THz-TDS и гиперспектральной технологии можно идентифицировать лиственные породы из разных семейств и родов с наивысшими показателями точности 92 и 94 %. Уровень распознавания THz-TDS для пяти образцов древесины хвойных пород из одного семейства 92 %, что является хорошим показателем, в то время как гиперспектральная технология не дает таких результатов.

Ключевые слова: *терагерцовая спектроскопия, гиперспектральная технология, метод опорных векторов, лиственная древесина, хвойная древесина.*

Introduction. Wood is a natural material that finds widespread use in various daily life fields, such as architecture, art, and furniture. Different wood species exhibit significant variations in properties, prices, and applications. Due to the vast diversity of wood species, modern identification procedures are necessary for the timber trade and wood processing industries. Currently, traditional methods for identifying wood species rely mainly on macroscopic observation, microscopic sectioning, DNA barcoding, and other techniques [1, 2]. However, these methods have several limitations. For instance, macroscopic observation requires highly skilled inspectors and has low detection efficiency, while microscopic sectioning and DNA barcoding are time-consuming, laborious, and can potentially damage the wood. Therefore, it is crucial to explore more efficient, rapid, non-destructive, and accurate methods for detecting and identifying wood species when traditional approaches fall short. Spectral analysis has emerged as a mature technique, providing advantages such as quick, precise, and non-destructive testing. The visible and near-infrared wavelengths in the electromagnetic spectrum are commonly used for wood detection, with near-infrared spectroscopy and hyperspectral imaging methods frequently applied [3–6]. These techniques have been widely utilized for non-destructive testing of wood in various applications [7–9].

Recently, researchers have shown a growing interest in exploring the terahertz (THz) waveband, the last frequency range in the electromagnetic spectrum. The primary chemical components of wood, cellulose, hemicellulose, and lignin, have vibrational and rotational energy levels with fixed frequencies in the THz range [10, 11]. THz spectroscopy can detect and identify these macromolecules by extracting their vibrational and rotational features, providing a specific identification spectrum for the molecular conformation [12]. In addition, wood is nearly transparent to the THz wave, in contrast to its low penetrability in the visible and near-infrared range. Therefore, it is feasible to collect characteristic data on the THz transmission spectrum of wood, which can be utilized to investigate its composition, structure, and physical and chemical properties. THz spectroscopy can be employed for the identification of wood species as a complementary technology to other spectral detection techniques such as infrared spectroscopy.

THz spectroscopy has been widely utilized in various fields, including the detection of pesticides, materials, and cancer tissues [13–17]. While using THz spectroscopy to identify wood is not a conventional practice, certain studies focused on predicting the physical properties of wood using THz spectroscopy have demonstrated its viability and superiority in wood detection [18–21]. In a recent study, we successfully identified five different species of redwood using THz time-domain spectroscopy (THz-TDS), namely *Dalbergia bariensis*, *Dalbergia oliveri*, *Bois de rose*, *Pterocarpus santalinus*, and *Dalbergia cochinchinensis* [22]. The results showed that THz-TDS performed remarkably well in identifying the wood species. However, there have been few reports comparing THz spectroscopy with other spectroscopic techniques for wood identification.

Support vector machine (SVM) is a robust machine learning algorithm that is capable of solving nonlinear classification problems and has demonstrated excellent performance in various fields [23–25]. SVM exhibits good generalization ability, particularly when dealing with small sample sizes, and effectively avoids overfitting and local minima problems that are common in neural networks [26].

We aimed to investigate the properties of five species of softwood and five species of hardwood using THz-TDS and hyperspectral techniques. We compared and analyzed the differences in spectral properties between softwood and hardwood and built SVM recognition models for identification. Our research provides a meaningful comparison between THz-TDS and hyperspectral techniques, which are significant for the nondestructive testing of wood.

Sample preparation. Ten wood species, including five species of softwood and five species of hardwood, were selected for this experiment. The hardwood species were *Xylosma racemosum*, *Populus davidiana*, *Fraxinus rhynchophylla*, *Betula platyphylla*, and *Tilia tuan Szyszyl*, while the softwood species were *Pinus sylvestris*, *Pinus tabulaeformis*, *Pinus massoniana*, *Larix gmelinii*, and *Pinus koraiensis*.

Wood chip samples measuring 50×50×5 mm were precisely cut from discs intercepted at breast height from the logs using cutting tools. A total of 400 experimental samples were prepared, with 40 samples cut for each of the ten wood species. The wood chip samples were kept in the same atmospheric environment to naturally dry to an air-dried state to prevent moisture from affecting the terahertz tests.

THz time-domain spectrum and hyperspectral image collection. The terahertz spectra of the wood samples were collected using a TERA K15 transmission terahertz spectrometer at the State Key Laboratory of Precision Measurement Technology and Instruments, Tianjin University [27]. The system generated a terahertz wave with an average power of 500 mW and a pulse width of less than 90 fs using a femtosecond laser pulse with a center wavelength of 1650 nm and a repetition frequency of 100 MHz. Prior to the scanning procedure, a set of reference spectra without samples was measured. The THz-TDS data for each sample were acquired three times, and the frequency domain spectra of the sample and reference signal were obtained by performing a fast Fourier transform (FFT) on the time-domain signal. The system had a sampling interval of 26 fs and a sampling duration of 80 ps. Throughout the experiment, the temperature and relative humidity were maintained at 25.5–27.6°C and 48.2 to 50%, respectively.

The hyperspectral imaging system used in this experiment was a SOC710VP portable hyperspectral imager, which had 128 bands, a spectral resolution of 1.3 nm, and a wavelength range of 400 to 1000 nm. The sample was positioned vertically in the middle of a SOC hard grey board, and the measurement was conducted with the lens aperture set at f 5.6. The hyperspectral image data of each sample was gathered by an imaging spectrometer.

THz optical parameter extraction. The THz-TDS can be used to calculate the absorption coefficient and refractive index, based on the optical constant extracting model proposed by Dorney and Duvillaret [28, 29].

The refractive index of the THz spectrum can be expressed as follows:

$$n(\omega) = \frac{\varphi(\omega)c}{\omega d} + 1. \quad (1)$$

The absorbance can be expressed as shown:

$$\alpha(\omega) = \frac{2}{d} \ln \frac{4n(\omega)}{\rho(\omega)\left(n(\omega)+1\right)^2}, \quad (2)$$

where $n(\omega)$ is the real part of the refractive index, d is the sample thickness, c is the velocity of the THz wave propagating in a vacuum, ω is the angular frequency, $\rho(\omega)$ and $\varphi(\omega)$ are the amplitude ratio and phase difference between the sample signal and the reference signal, respectively.

Hyperspectral image calibration and region of interest (ROI) extraction. Initial image correction was performed using the SRAnal710 software of the SOC710VP portable hyperspectral imager. Raw hyperspectral reflectance images were normalized into relative hyperspectral reflectance images using white reference and dark reference images to reduce signal noise caused by changes in equipment structure and detector sensitivity [30].

In this study, a region of interest (ROI) was set as a 50×50 square area in the center of each sample's image. The average reflectance spectrum value of each pixel within the ROI was then extracted as the sample's average spectral data, resulting in a total of 400 average spectral data.

Result and discussion. Figure 1 illustrates the absorption coefficient spectra for different softwood and hardwood species. The primary differences among the five softwood species were the intensity and location of the absorption peak in the frequency range of 0.2 to 2.0 THz. The absorption coefficient spectra of the five softwood species exhibited significant variations from 0.2 to 1.2 THz. The most prominent distinction was the varying strength of the absorption coefficients among the five softwood species, with *Larix gmelinii* having the highest intensity, followed by *Pinus massoniana*, *Pinus koraiensis*, *Pinus tabulaeformis*, and *Pinus sylvestris*. *Pinus massoniana* exhibited four absorption peaks (0.56, 0.93, 1, and 1.1 THz), *Pinus sylvestris* showed three (0.56, 1.11, and 1.18 THz), *Pinus tabulaeformis* had five (0.56, 0.94, 1.0, 1.11, and 1.19 THz), *Larix gmelinii* had four (0.79, 0.86, 0.95, and 1.0 THz), and *Pinus koraiensis* had three (0.56, 1.0, and 1.11 THz). The differences among the absorption peaks of the five softwood species were noticeable. The absorption coefficient spectra of the five softwood species exhibited greater overlap beyond 1.20 THz, and the differences were negligible. For subsequent data processing and modeling, the spectrum data in the 0.2 to 1.2 THz region were chosen.

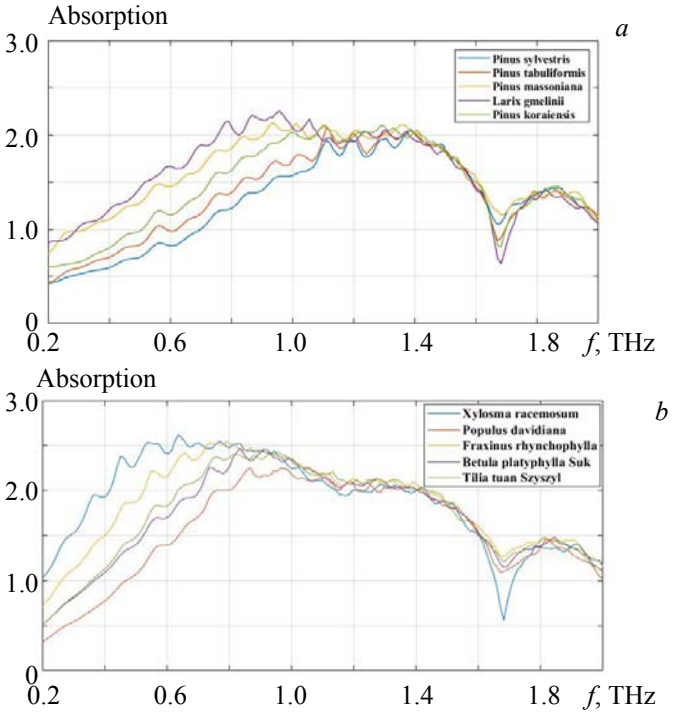

Fig. 1. Terahertz absorption spectra of five softwoods (a) and five hardwoods (b).

The absorption coefficient spectrum waveforms of the five hardwood species from 0.2 to 1 THz were highly diverse, primarily due to their various absorption coefficient intensities and locations. *Xylosma racemosum* was the most intense, followed by *Fraxinus rhynchophylla*, *Tilia tuan Szyszyl*, *Betula platyphylla*, and *Populus davidiana*. *Xylosma racemosum* had three main absorption peaks (0.45, 0.63, and 0.76 THz), *Populus davidiana* had two main absorption peaks (0.86 and 0.96 THz), *Fraxinus rhynchophylla* had two main absorption peaks (0.54 and 0.65 THz), *Tilia tuan Szyszyl* had four main absorption peaks (0.75, 0.81, 0.87, and 0.95 THz), and *Betula platyphylla* had three main absorption peaks (0.73, 0.83, and 0.98 THz). The primary absorption peak positions varied from 0.2 to 0.8 THz for *Xylosma racemosum* and *Fraxinus rhynchophylla*, and from 0.7 to 1.0 THz for *Populus davidiana*, *Betula platyphylla*, and *Tilia tuan Szyszyl*. The absorption coefficient spectra of the five hardwood species showed the most overlap after 1.0 THz. Consequently, spectra within the range of 0.2 to 1.0 THz were chosen for post-data processing and modeling.

Figure 2 depicts the original spectral characteristic curves of softwood and hardwood species based on their hyperspectral reflectance. It is notable that the five species of softwood exhibited similar tendencies in their reflectance spectrum curves, with a respective reflectance threshold range of 0.09 to 1.00. *Pinus sylvestris*, *Pinus tabulaeformis*, *Pinus massoniana*, and *Pinus koraiensis* demonstrated a high degree of resemblance, making it difficult to distinguish them in terms of reflection waveform and intensity. However, differentiating *Larix gmelinii* from the other four pine varieties was straightforward, as it exhibited a distinct difference in reflectance intensity. The fact that *Larix gmelinii* belonged to the genus *Larix* in the *Pinaceae* family provided a proper explanation. It is credible that the differences in its physical, chemical, and microstructural characteristics contributed to its unique spectrum compared to other *Pinus* species.

While the five hardwood species shared comparable peaks, troughs, and the direction of their reflectance spectrum curves, the reflectance intensity of the five hardwood species varied significantly. The five different types of wood exhibited similar overall trends in their visible-near infrared spectra, indicating that the fundamental chemical elements of each type of tree were essentially the same. The levels of reflectance among the five hardwood species in the visible light range of 400–727 nm were as follows: *Betula platyphylla* > *Populus davidiana* > *Fraxinus rhynchophylla* > *Tila tuan Szyszyl* > *Xylosma racemosum*. The visible spectrum was the predominant absorption region of the pigment composition, and variations in the composition and amount of pigment in the wood samples resulted in differences in the visible spectrum's absorption response in various wood types. To ensure that no valid information in the infrared band was lost, the 400–1000 nm band was used for the modeling study.

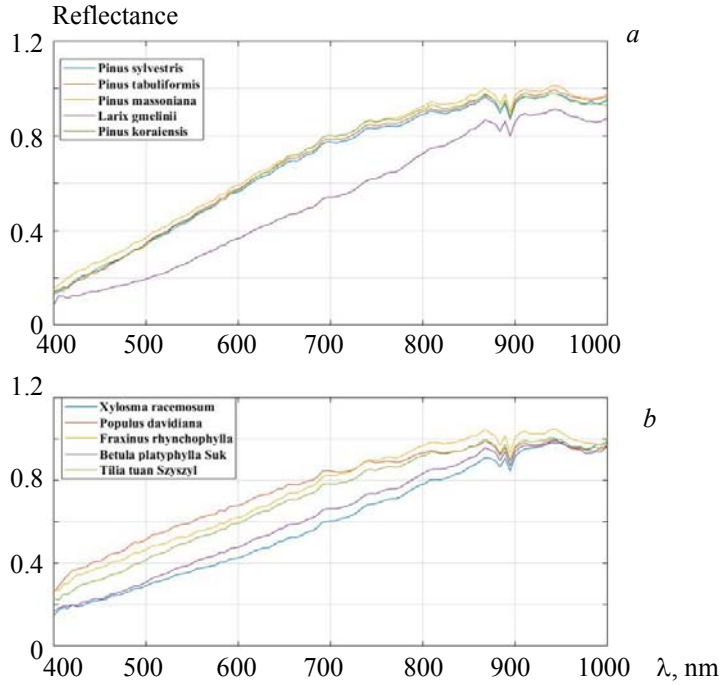

Fig. 2. Hyperspectral reflectance spectrum of five softwoods (a) and five hardwoods (b).

The study utilized spectrum data on ten wood species' terahertz absorption coefficients and hyperspectral data across the entire waveband. Preprocessing was conducted using three approaches: Savitsky–Golay (SG), standard normal variable transformation (SNV), and multivariate scattering correction (MSC). SVM recognition models were developed using both the original and preprocessed spectral data from the three approaches. The data were randomly split into training and test sets at a 3:1 ratio prior to modeling. The penalty factor parameter *C* and kernel function parameter g of the model were calculated using the grid method, with a linear kernel function employed for the kernel function.

Table 1 presents the recognition rates for the five categories of softwood absorption coefficients based on the SVM model created using the linear kernel function. The preprocessed spectral data model outperformed the original spectral data model, with the SNV-preprocessed model achieving the highest total recognition rate of 92%. All five species of pine wood exhibited recognition rates above 85%.

TABLE 1. Classification Results of THz Absorption Coefficients of Five Softwoods (Recognition rate of SVM/%)

Wood species	*Pinus sylvestris*	*Pinus tabuliformis*	*Pinus massoniana*	*Larix gmelinii*	*Pinus koraiensis*	Total recognition rate, %
Original	100	100	69.2	100	77.8	88
SG	90	100	93.3	71.4	78.6	90
SNV	100	92.3	83.3	100	88.9	92
MSC	94.4	87.5	75	100	87.5	90

The recognition rates of the SVM model using hyperspectral reflectance data from five softwood species are presented in Table 2. The preprocessed data model did not exhibit a significant improvement in recognition accuracy compared to the original spectral data model. The model's recognition accuracy ranged from 50 to 62%, which did not yield satisfactory results.

Table 3 presents the total recognition rates of the SVM hardwood classification models after preprocessing with SG, SNV, and MSC methods. The results showed that all models achieved recognition rates higher than 80%, indicating that proper preprocessing improved the classification model’s overall performance. Notably, the SNV-SVM model had the highest recognition rate among all models. The SNV preprocessing increased the SVM hardwood classification model’s overall recognition rate by 12% compared to the

model without preprocessing. This result emphasizes the importance of optimizing the model through appropriate preprocessing techniques.

TABLE 2. Classification Results of the Hyperspectral Reflectance of Five Softwoods (Recognition rate of SVM/%)

Wood species	*Pinus sylvestris*	*Pinus tabuliformis*	*Pinus massoniana*	*Larix gmelinii*	*Pinus koraiensis*	Total recognition rate, %
Original	26.7	57.1	25	90.9	55.5	50
SG	76.7	63.6	60	83.3	81.8	58
SNV	12.5	55.6	44.4	66.7	66.7	52
MSC	55.6	37.5	50	100	60	62

TABLE 3. Classification Results of THz Absorption Coefficients of Five Kinds of Hardwoods (Recognition rate of SVM/%)

Wood species	*Xylosma racemosum*	*Populus davidiana*	*Fraxinus rhynchophylla*	*Betula platyphylla Suk*	*Tilia tuan Szyszyl.*	Total recognition rate, %
Original	93.7	83.3	84.6	50	75	80
SG	100	87.5	80	77	72.7	82
SNV	100	100	70	90	100	92
MSC	100	100	80	70	80	86

TABLE 4. Classification Results of the Hyperspectral Reflectance of Five Hardwoods (Recognition rate of SVM/%)

Wood species	*Xylosma racemosum*	*Populus davidiana*	*Fraxinus rhynchophylla*	*Betula platyphylla Suk*	*Tilia tuan Szyszyl.*	Total recognition rate, %
Original	85.7	87.5	100	92.3	63.6	86
SG	90.9	100	78.5	100	88.9	90
SNV	100	100	100	100	75	94
MSC	100	100	85.7	100	61.5	88

Table 4 presents the recognition rates of the SVM model using data from five hardwood hyperspectral reflectance. The overall recognition rates of the hardwood were higher after adequate preprocessing (SG, SNV, and MSC) compared to those without preprocessing. Among them, the SNV-SVM was the most effective after preprocessing, with an overall identification rate of 94%. After SNV preprocessing, the SVM hardwood classification model's overall recognition rate increased by 8%.

The visible and near-infrared spectra of the five softwood species generally exhibited similar patterns, and they also had similar main chemical compositions since the primary spectral region of absorption for pigments is in the visible range. However, variations in the pigment level and composition of the samples led to differences in wood absorption in the visible spectrum region. The four pine species belonging to the same family and genus were challenging to identify in the visible-near-infrared spectral range, which resulted in a low overall recognition rate for the model. However, *Larix gmelinii*, a species in the genus *Larix*, could be easily distinguished from the other four pine species, and its recognition rate in the model was higher. This may be because the pigment content of *Larix gmelinii* was significantly different from that of the other four pine species.

Analysis of the absorption coefficient spectrum in the terahertz band enables better differentiation among the five species of softwood, with absorption peaks that are relatively identical in position but notably different in strength. The SVM model of softwood created using terahertz absorption coefficients after SNV preprocessing achieved a higher identification rate. The five species of hardwood belong to five separate families and vary in microstructure and physicochemical characteristics. While the SVM models of hardwood created from these two spectra can obtain reasonable recognition results in the terahertz and visible/near-infrared bands, they are poor recognition results for certain woods, indicating a need for further feature extraction from the spectral data.

Conclusions. Three spectral preprocessing methods were utilized for wood identification using terahertz time-domain spectroscopy and hyperspectral methods. The study involved preprocessing the hyperspectral reflectance and terahertz absorption coefficient data of wood samples, creating a support vector machine model for recognition, and comparing the recognition outcomes of the models. The results showed that the five species of softwood from the same family had similar hyperspectral reflectance curves in the visible and near-infrared bands, leading to subpar overall recognition performance of the hyperspectral model. On the other hand, terahertz time-domain spectroscopy was a better option for identifying the five softwood species. The spectral characteristics of the five hardwood species in different families and genera varied greatly. Although both hyperspectral spectroscopy and terahertz spectroscopy could successfully identify the hardwood species, there were issues with identifying specific hardwood species. To improve identification results, the next stage of work will focus on extracting features from the wood spectra.

REFERENCES

1. E. A. Wheeler, P. Baas, *IAWA J.*, **19**, No. 3, 241–264 (1998).
2. M. Yu, K. Liu, L. Zhou, L. Zhao, S. Q. Liu, *Holzforschung*, **70**, No. 2, 127–136 (2016).
3. L. Pang, J. Xiao, J. J. Ma, L. Yan, *J. For. Res.*, **32**, No. 2, 461–469 (2021).
4. V. Shenbaga Priya, D. Ramyachitra, *Cluster. Comp.*, **22**, No. S6, 13569–13581 (2019).
5. G. J. Qiu, E. L. Lu, H. Z. Lu, S. Xu, F. G. Zeng, Q. Shui, *Sensors*, **18**, No. 4, 1010–1025 (2018).
6. J. Sun, Y. C. Zhang, H. P. Mao, S. L. Cong, X. H. Wu, P. Wang, *Optik*, **153**, 156–163 (2018).
7. S. Nisgoski, A. A. de Oliveira, G. I. B. de Muñiz, *Wood. Sci. Technol.*, **51**, No. 4, 929–942 (2017).
8. G. Y. Shi, J. Cao, C. Li, Y. L. Liang, *J. For. Res.*, **31**, No. 3, 1061–1069 (2020).
9. L. Yu, Y. L. Liang, Y. Z. Zhang, J. Cao, *J. For. Res.*, **31**, No. 3, 1053–1060 (2020).
10. M. Peccianti, R. Fastampa, A. M. Conte, O. Pulci, C. Violante, J. Łojewska, M. Clerici, R. Morandotti, M. Missori, *Phys. Rev. Appl.*, **7**, No. 6, 064019 (2017).
11. T. Trafela, M. Mizuno, K. Fukunaga, M. Strlič, *Appl. Phys. A Mater.*, **111**, No. 1, 83–90 (2013).
12. F. S. Vieira, C. Pasquini, *Anal. Chem.*, **86**, No. 8, 3780–3786 (2014).
13. M. Naftaly, R. E. Miles, *IEEE*, **95**, No. 8, 1658–1665 (2007).
14. K. Okada, Q. Cassar, H. Murakami, G. MacGrogan, J. P. Guillet, P. Mounaix, M. Tonouchi, K. Serita, *Photonics*, **8**, No. 5, 151 (2021).
15. F. F. Qu, L. Lin, Y. He, P. C. Nie, C. Y. Cai, T. Dong, Y. Pan, Y. Tang, S. M. Luo, *Molecules*, **23**, No. 7, 1607 (2018).
16. S. Tsuzuki, N. Kuzuu, H. Horikoshi, K. Saito, K. Yamamoto, M. Tani, *Appl. Phys. Express*, **8**, No. 7, 072402 (2015).
17. H. Wang, Y. Horikawa, S. Tsuchikawa, T. Inagaki, *Cellulose*, **27**, No. 17, 9767–9777 (2020).
18. T. Inagaki, I. D. Hartley, S. Tsuchikawa, M. Reid, *Holzforschung*, **68**, No. 1, 61–68 (2014).
19. K. Krügener, S. Sommer, E. Stübling, R. Jachim, M. Koch, W. Viöl, *J. Infrared. Millim. Terahertz. Waves*, **40**, No. 7, 770–774 (2019).
20. M. Reid, R. Fedosejevs, *Appl. Opt.*, **45**, No. 12, 2766–2772 (2006).
21. S. Tanaka, K. Shiraga, Y. Ogawa, Y. Fujii, S. Okumura, *J. Wood. Sci.*, **60**, No. 2, 111–116 (2014).
22. Y. Wang, S. She, N. Zhou, P. X. Jia, J. G. Zhang, *Spectrosc. Spectr. Anal.*, **39**, No. 9, 2719–2724 (2019).
23. A. Subasi, *Comp. Biol. Med.*, **43**, No. 5, 576–586 (2013).
24. R. Pouteau, A. Collin, *Remote Sens. Lett.*, **4**, No. 7, 686–695 (2013).
25. C. M. Salvador, C. C. K. Chou, *Atm. Environ.*, **95**, 288–295 (2014).
26. J. W. Zhang, W. L. Song, B. Jiang, M. B. Li, *J. For. Res.*, **29**, No. 2, 557–564 (2018).
27. Y. Wang, S. She, N. Zhou, J. G. Zhang, H. Yan, W. B. Li, *Bioresources*, **14**, No. 1, 1033–1048 (2019).
28. T. D. Dorney, R. G. Baraniuk, D. M. Mittleman, *J. Opt. Soc. Am. A*, **18**, No. 7, 1562–1571 (2001).
29. L. Duvillaret, F. Garet, J. L. Coutaz, *Appl. Opt.*, **38**, No. 2, 409–415 (1999).
30. M. Kamruzzaman, Y. Makino, S. Oshita, *J. Food. Eng.*, **170**, 8–15 (2016).